

NEW DEVELOPMENT IN HIGH RESOLUTION ACOUSTIC IMAGING FOR MATERIALS EVALUATION

Roman Gr. Maev

DaimlerChrysler/NSERC Industrial Research Chair in Applied
Solid State Physics and Material Characterization,
University of Windsor, Ontario, N9B 3P4, Canada
maev@uwindsor.ca

Abstract

This review describes recent advances in high-resolution acoustical imaging and quantitative acoustic microscopy for material evaluation. The theoretical basis, as well as experimental fundamentals for quantitative characterization of the contrast response in the acoustic microscope, will be described. Together with the well known $V(z)$ method, new techniques for the measurement of acoustical parameters will be discussed. This will include the $V(x, t)$ method, ultrasonic micro-spectrometry, air-coupling pair measurement technique for the reflection mode, as well as the $A(z)$ method for the transmission mode. Improvement of imaging resolution using higher harmonics is one of the priorities to be addressed, including new opportunities for non-linear material characterization using parametric acoustic imaging. The last part of review is related to recent developments of high-resolution imaging techniques for practical uses. Based on the most successful experimental results, some examples will be provided of different applications, including evaluation of advanced material structure, quality control of joints, adhesive bonding, and layer structures.

Introduction

The most popular quantitative technique in acoustic microscopy is the $V(z)$ method [1, 2], in which the acoustic velocity and attenuation of leaky surface acoustic waves, as well as a reflectance function, can be determined from the output signal V of the transducer, acquired as a function of the specimen displacement z . Together with the well known $V(z)$ method, we will introduce other techniques for the measurement of acoustical parameters. For quantitative materials characterization, acoustic methods employing separated transmitting and receiving transducers were developed, such as an ultrasonic micro-spectrometer with spherical-planar-pair lenses for the measurement of the reflection coefficient [3, 4]. The angular spectrum of the reflected wave in such system is determined by the rotation of the lens system as a whole, relative to the specimen surface. The ultrasonic system with two transducers was also used for a measurement of the resonant transmission coefficient, [5] and for the determination of Lamb dispersion curves [6].

Obtaining the required data for the reconstruction algorithms occurred in two ways: one, the voltage of the output transducer was measured as a function of the lateral displacement of the transducer on the specimen's surface; or two, as a function of the frequency of the probing electrical tone burst pulse. A two-dimensional recording of the wave, scattered by the specimen, was proposed [7] for measuring elastic constants. The focus of the transmitting transducer in this method is placed on the specimen surface, but the scan plane of the receiver is located far from the focus. Thus, the recorded spatial distribution represents the angular spectrum of the reflected or transmitted wave. The angular resolution of the methods is determined by the spatial resolution of the receiver and the distance between the scan plane and focus. In previous articles [8, 9] we developed a new technique for measuring acoustical parameters called the $A(z)$ method for the transmission mode. A new $V(x)$ method was introduced later for the reflection mode [10, 11]. Both the $A(z)$ and $V(x)$ methods may include additional options, based on the air-coupling pair measurement technique for both the reflection mode, and for the transmission mode.

$V(Z)$ Method

The most popular quantitative technique in acoustic microscopy is the $V(z)$ method, in which the acoustic velocity and attenuation of leaky surface acoustic waves, as well as a reflectance function, can be determined from the output signal V of the transducer acquired as a function of specimen displacement z . In most of these systems, the output voltage $V(z)$ of the focused transducer is recorded as a function of the distance between the focus and the surface of the specimen [1, 2] and [12–15]. The phase velocity and propagation attenuation of leaky surface acoustic waves (LSAW), as well as a reflectance function for the specimen-liquid coupling interface, can be obtained from the recorded amplitude data. In the $V(z)$ system (Fig. 1a), the LSAW is generated by a ray incident on the liquid-solid interface at the critical angle θ_R . The surface wave propagates along the interface reradiating ("leaking") back to the liquid at the same angle θ_R . If the transducer is moved toward the specimen, one of the reradiated rays (ray R) is effectively received by the transducer. Only a leaky wave whose critical angle is less than the half-aperture

angle of the transducer $\theta_R < \theta_m$ can be excited and detected in this scheme.

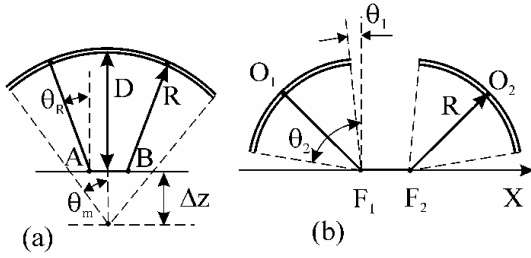


Figure 1. Ray models of the (a) $V(z)$ and (b) $V(x)$ material characterization systems

The time delay Δt between the responses to the ray R and the directly reflected ray D is related to the velocity of the LSAW, C_R [16, 17]:

$$C_R = \left[\frac{\Delta t}{C \cdot \Delta z} - \frac{1}{4} \cdot \left(\frac{\Delta t}{\Delta z} \right)^2 \right]^{-1/2},$$

where C is the sound velocity in the liquid and Δz is the defocusing distance. Obviously, the accuracy of the LSAW measurement increases with increasing Δz . The maximum value of Δz is limited by the focal distance F of the lens and the half-aperture angle θ_m : $\Delta z < F \cdot \cos(\theta_m)$. Usually, the maximum value of F is limited by the sound attenuation in the liquid. On the other hand, it is possible to obtain better accuracy by decreasing θ_m , but this is not desirable because of the reduction in the critical angle range.

A point-focus-beam acoustic lens was used in the first implementation of the $V(z)$ technique for an isotropic specimen study [2]. For the characterization of anisotropic materials, a line-focus-beam acoustic lens was proposed [12]. A Lamb wave lens and directional lenses with noncircular shaped transducers [13] were developed to obtain enhanced sensitivity for particular ranges of incident or orientation angles. As well, various electrical exciting waveforms and processing electronics were employed for $V(z)$ data acquisition. The conventional UMC system works in a tone burst mode and the amplitude of $V(z)$ is only used for analysis. The amplitude and the phase of the output voltage were recorded to reconstruct the reflectance function by the Fourier transform of the complex $V(z)$ [14]. A continuous wave Doppler system produces a complex $V(z)$ for a single, particular frequency [10, 18]. Conversely, the $V(z, t)$ waveform acquired in the pulse mode represents the properties of the specimen over a wide frequency band [19, 20].

With all of these techniques, the accuracy of the measured LSAW parameters and the incident angle resolution increases with the growing amount of $V(z)$

data [14]. However, the maximal defocusing distance is limited in the $V(z)$ configuration by the geometry of the acoustic lens. Furthermore, the wave velocity in water is used as reference in the $V(z)$ schemes. Due to the temperature dependence of the wave velocity in water, the error in the temperature measurement significantly affects the accuracy of the measured velocity and attenuation of LSAW [1, 15, and 29].

Micro-Spectrometry

Several ultrasonic systems employing two transducers have also been developed for quantitative material characterization. In an ultrasonic micro-spectrometer, spherical-planar-pair lenses were used for the measurement of the reflection coefficient over a wide frequency range [3], [4]. An angular spectrum of the reflected wave is detected in this system by tilting the spherical-planar-pair lenses as a unit. The size of the planar transducer is large enough to provide sufficient angular selectivity and, because of geometrical restrictions, the measurements can not be carried out at small and large angles of incidence (see Figure 2).

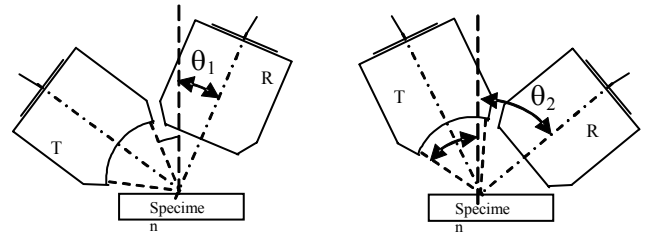


Figure 2. Experimental setup for ultrasonic angular micro-spectrometer with Spherical-Planar Pair lenses. Incident angle $\theta_1 < \theta < \theta_2$.

An ultrasonic system employing separated transmitting and receiving point-focus transducers has been developed to study the anisotropic propagation of LSAW. During the experiments [21, 22], the foci were located on the surface of the specimen at a fixed distance, and the specimen was rotated to obtain the group velocity of surface waves as a function of the propagation angle. In systems [23]–[24], the focus of the transmitter was located on the liquid–solid interface, but the recording of the scattered acoustic field was carried out by two-dimensional scanning of the receiving transducer. The recorded spatial distribution represented the angular spectrum of the scattered wave associated with the reflectance or transmission coefficients. Thus, using this technique, the angular resolution was restricted by the spatial resolution of the receiver and the distance from the point source to the plane of the data acquisition.

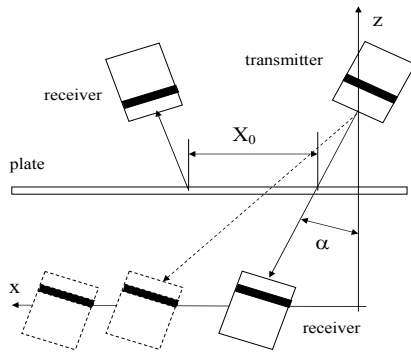


Figure 3. Experimental setup for air coupling pair system. Due to the narrow directivity of the transducers, additional monitoring of angle α is used

The ultrasonic system with two transducers was also used for a resonant transmission coefficient measurement and for the determination of Lamb dispersion curves [6]. Lateral scanning of the receiving air coupling transducers along with surface of the specimen was used to acquire Lamb wave measurements and to study the properties of the materials in plate form.[5, 25](see Figures 3 and 4). Obtaining the required data for the reconstruction algorithms occurred in two ways, one—the voltage of the output transducer was measured as a function of the lateral displacement of the transducer on the specimen's surface, or two—as a function of the frequency of the probing electrical tone burst pulse. However, the transducers had narrow directivity functions and monitoring of the transducer angles was employed to acquire a complete data set. A two-dimensional recording of the wave, scattered by the specimen, was proposed for measuring elastic constants in papers [7]. A two-dimensional Fourier transformation of the acquired time-spatial data represented the wave number dispersion curves. Due to the high directivity of the transducers employed in the experiments, the single scan data corresponds to a narrow range of the angles of incidence. To obtain dispersion curves for the entire angular range, the data acquisition and processing should be repeated many

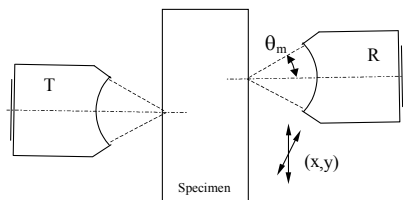


Figure 5. Through transmission mode. The angular resolution in this method is determined by the spatial resolution of the receiver and the distance between scan plane and focus. The incident angle is $\theta < \theta_m$

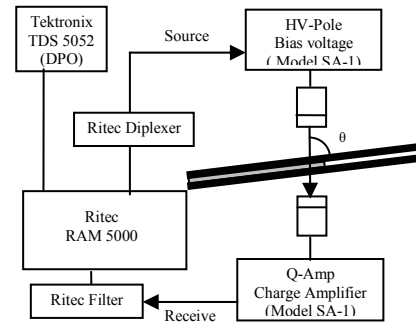


Figure 4. Air-Coupling pair measurements. The lap joints are placed in between the transducers with angle $\theta = 8^\circ - 12^\circ$. Frequency of burst is equal 500 kHz

times at different angular orientations of the transducers (Figure 5). Another system with highly focused probes has been developed for rapid dispersion curve mapping [23] [24], because of the large angular aperture of the transducers, only a single scan is necessary to acquire the complete data set.

The A(z) Method

The A(z) method relies on the dependence of the output signal A(z) on the distance z between the receiving and radiating lenses in the two-lens focusing system of the transmission acoustic microscope [8,9]. Without an object the output signal is at its maximum when the focuses of both lenses coincide (confocal position). Displacing one of the lenses causes signal decay and oscillations due to the interference of the signals produced by different parts of the beam in the receiving transducer (Figure 6). When an object such as a plate with thickness d, is placed in the path of the focused beam, its focus is shifted due to the refraction of a convergent beam in the plate. To reach the maximum of the signal, it is necessary to change the distance between the lenses. A maximum arises with a new confocal position (Figure 6). Applying a well-known formula of the ray optics the lens shift z can be expressed as: $z = d(1 - C_L/C)$, where C_L and C are ultrasound velocities in an object and in a coupling liquid, respectively. Measuring the specimen thickness d and the shift z of the receiving lens, we can determine the ratio C_L/C and, finally, a value of C_L . Measuring the ratio of maximums on both of the A(z) plots, before placing an object and after it, makes it possible to find a value of the transmission coefficient and then to estimate the attenuation in a specimen. An earlier theoretical model for the A(z) method was developed in [9] and experimentally this method has been applied to measuring acoustic parameters of some polymer, polymer blends (see Figure 9) and biological samples [8].

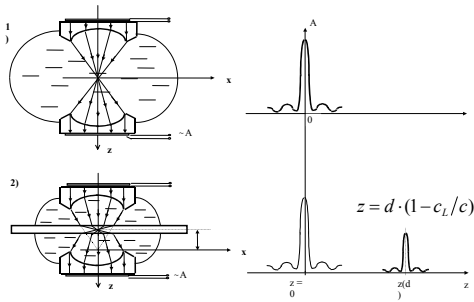


Figure 6. A(z) method for quantitative measurements in through transmission

V(x, t) Method

$V(x, t)$ is a newly developed time-resolved, pair lenses, line-focused method based on the lateral scanning of the receiving transducer. It was shown theoretically [10, 11] that the output voltage $V(x, t)$ of the system is related by the Fourier transform to the product of the reflectance coefficient and the transfer function. In the $V(x)$ scheme, the tilted transmitting and receiving transducers are used in a pitch-catch arrangement, and the receiver is translated along the interface in the x direction (Figure 1, (b)). The velocity of the non dispersive LSAW is simply the ratio of the travel distance Δx and the relative time delay Δt of the leaky wave R : $C_R = \Delta x / \Delta t$. Due to the geometry of the $V(x)$ system, the range of angles of incidence (θ_1, θ_2) can be made close to the values $(0, \pi/2)$, and there is no restriction on the maximum scanning distance Δx in the direction of the LSAW propagation.

For an ideal uniform temperature distribution in the immersion liquid (see Figure 8), the time of flight in the liquid $\Delta t^* = (O_1F_1 + F_2O_2) / C$ is constant during data acquisition. Also, Δt^* remains constant if the temperature distribution along the rays O_1F_1 and F_2O_2 does not change during the scan of the receiving transducer. Under this sufficient condition, the relative time delay Δt is only associated with the LSAW velocity, and the temperature coefficient ηx of the CR measurement error is negligible. It is difficult to estimate theoretically the value of ηx , but below we have presented the results of the experimental study of the temperature stability of the $V(x)$ scheme.

The proposed method was illustrated experi-

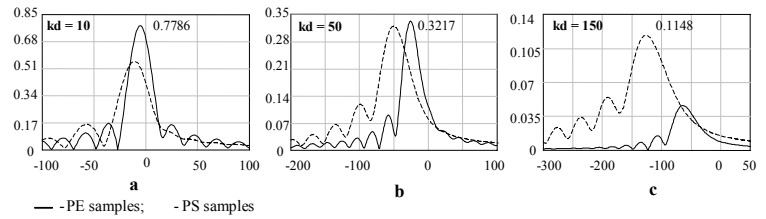


Figure 7. Application of A(z) method for polymer study: $A(kz)$ curves for polyethylene and polystyrene samples with thickness $kd = 10$ (a), $kd = 50$ (b) and $kd = 150$ (c). The peak shift from the point of $z = 0$ is proportional to the specimen thickness d and depends on the sound velocity ratio – the larger the shift, the bigger the ratio.

mentally by measurements of the velocities of leaky Rayleigh, Lamb, and longitudinal skimming waves [28]. Some results for the materials with known properties were tested using the experimental setup described in Figure 8, 9. The complex reflectance function for the water-lead interface is similar for all angles of incidence because of the high density and low elasticity of lead. In previous work, [11, 28] a new time-resolved, line-focused UMC system was developed based on lateral scanning of the receiving transducer; it was shown theoretically that the output voltage $V(x, t)$ of the system is related by the Fourier transform to the product of the reflectance coefficient and the transfer function. In comparison with the $V(z)$ system, the geometry of the $V(x)$ scheme does not restrict the scanning distance and the aperture angle. The measurements of the LSAW velocity carried out using fused quartz over a wide temperature range show good temperature stability of the measurements employing the $V(x)$ technique. The angular resolution of the $V(x, t)$ system was analyzed using the ray model and wave theory. In comparison with the $V(z)$ system, the geometry of the $V(x)$ scheme does not restrict the scanning distance and the aperture angle. The proposed method was illustrated experimentally by measurements of the velocities of leaky Rayleigh, Lamb, and longitudinal skimming waves. The experimental results obtained for the metal, crystal, ceramic, and polymer specimens are in good agreement with published data. The measurements of the LSAW velocity carried out using fused quartz over a wide temperature range show good temperature stability of the measurements employing the $V(x)$ technique.

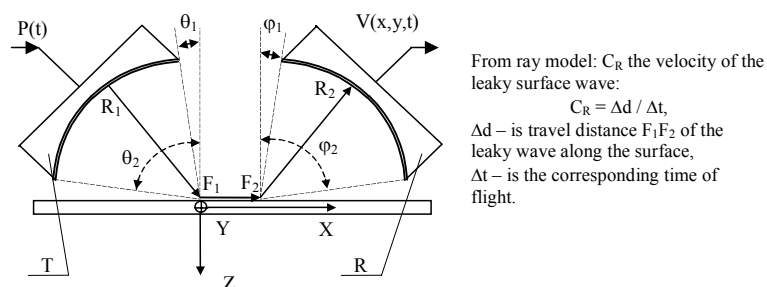


Figure 8. Physical principles of $V(x, t)$ method

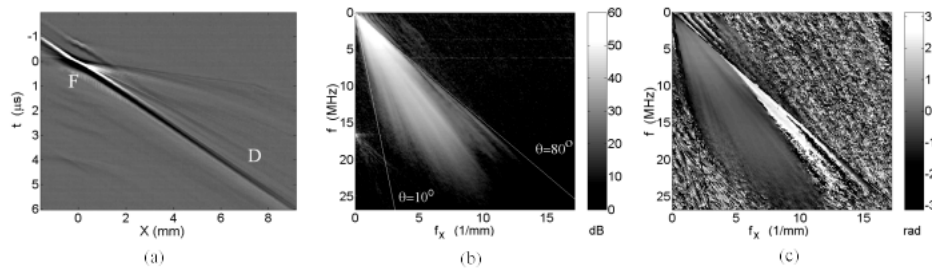


Figure 9. The $V(x, t)$ waveform recorded for lead (a), and the magnitude (b) and phase (c) of the spectrum of $V(x, t)$. Markers F and D correspond to the focused and defocused positions of the transducers, respectively.

Second harmonic mode of the acoustical microscope

The signal of the second harmonic, generated by nonlinear reflection, in most cases is 30–50 dB weaker than the signal of fundamental frequency, requiring careful selection of the experimental parameters. A single, short sound pulse is usually used in the acoustical microscope to maximize the spatial resolution. The wide-band spectrum of such a pulse contains strong components at double frequency. As well, the bulk nonlinearity of all the acoustical components of the microscope and object, especially of the coupling liquid, produce uninteresting second harmonic waves, which accompany the waves of the fundamental frequency. These waves will therefore contribute to the image at second harmonic, identical information to that already found in the linear picture [19]. In [20] this idea was experimentally demonstrated for the resolution of weak-reflecting inclusions, using a scanning microscope with a 25 MHz acoustical focusing lens. A selective filter-amplifier with a basic frequency of 50 MHz and a bandwidth 4 MHz was included into the receiving branch (see. Figure 7).

The sound wave was excited by applying to the lens transducer a single pulse with amplitude of 120 V and duration of 16 nS. Without taking any specific action to enhance the second harmonic, its level in the received signal lies at approximately 25 dB (measured during reflection from the surface of a steel plate in beam focus). By decreasing the receiver bandwidth, the tone burst of the second harmonic has a significantly longer duration compared to that without frequency selection. This leads to the deterioration of the spatial resolution in depth up to 0.5–0.7 mm.

The C-scan image is generated by mechanical raster scanning of an area up to 40×40 mm along the surface with steps of 0.05–0.01 mm. Figure 11 presents the scans of such a specimen: two galvanized steel sheets with thickness 2 mm, joined by a resistance spot weld. To exclude any aberration due to non-planar surface conditions, the indentation from the weld electrode was removed by milling. The dark spot in center of the pictures is the weld nugget. The

sound can freely pass through it and only some reflecting inhomogeneities are visible as light points.

The bright area outside the weld corresponds to the free internal surface of the upper sheet with practically 100% sound reflection. Between these regions lies a gray ring, corresponding to a zone with poor acoustical contact. It is known that in this zone melted zinc accumulates during the welding process, and creates a lot of connecting stalactite-stalagmite type structures. Such a microrough connective layer should be a very good source of contact acoustical nonlinearity. Since the thickness of this layer and the size of these microstructures are much less than a wavelength, they will contribute in an integral way. Indeed, the second harmonic picture shows this region as a bright white ring. The amplitude of the second harmonic in this region is at least ten times bigger than that of the other regions.

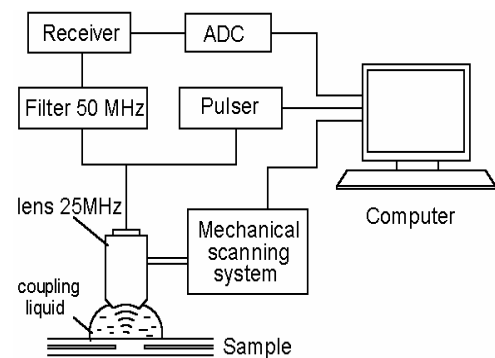


Figure 10. Schematic diagram of the scanning acoustical microscope as used for second harmonic imaging

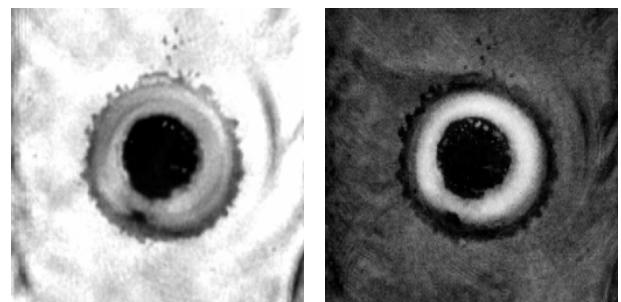


Figure 11. C-scans of spot weld, obtained on fundamental frequency (left) and on second harmonic (right). Size of scanned region is 12×12 mm.

Conclusion

During the last few decades, the acoustic microscope has become a common instrument for the investigation of the internal structure of materials and for industrial non-destructive evaluation. At the same time, quantitative acoustic imaging research was mostly applied in high resolution acoustic microscopy in material sciences and also in biomedical imaging. Further improvement of the quantitative methods may be realized using other types of ultrasonic-media interactions and, accordingly, provide additional specific information about the object. The realization of these methods will constitute a considerable and exciting expansion in the applicability of the acoustic microscope. The quantitative NDE acoustical imaging technique and methods would enhance its capability for the material characterization and imaging of cracked micro-inhomogeneities, crucial for the integrity of high-damage risk materials and products used in NDE aviation technology, automotive and nuclear power industries as well as microelectronics.

Acknowledgment

I acknowledge the National Science and Engineering Research Council Canada (NSERC) and Daimler-Chrysler Corporation for funding this work. I would also like to thank my colleagues from other research groups, whose results were included in this review paper (see references), in particular I would like to thank my research associates for their help and significant contribution to this review paper, including my research associates Drs. S. Titov, F. Severin, E. Maeva, V. Levin, and many of my students and PDF.

References

- [1] A. Briggs, *Acoustic microscopy*, Oxford, Clarendon Press, 105–152, 1992.
- [2] R. Weglein and R. Wilson, “Characteristic material signature by acoustic microscopy”, *Electron. Lett.*, 14, 352–354, 1978.
- [3] N. Nakaso, K. Ohira, M. Yanaka Y. Tsukahara, “Measurement of acoustic reflection coefficients by an ultrasonic microspectrometer”, *IEEE Trans. Ultrason. Ferroelec. Freq. Contr.*, 41, 494–502, 1994.
- [4] N. Nakaso, Y. Tsukahara and N. Chubachi, “Evaluation of spatial resolution of spherical–planar–pair lenses for elasticity measurement with microscopic resolution”, *IEEE Trans. Ultrason. Ferroelec. Freq. Contr.*, 43, 422–427, 1996.
- [5] O. Lobkis, D. Chimenti, “Three–dimensional transducer voltage in anisotropic materials characterization”, *J. Acoust. Soc. Amer.*, 106, 36–45, 1999.
- [6] T. Kundu, A. Maji, T. Ghosh, and K. Maslov, “Detection of kissing bonds by Lamb waves”, *Ultrasonics*, 35, 573–580, 1998.
- [7] R. Smith, D. Sinclair and H. Wickramasinghe, “Acoustic microscopy of elastic constants” in *Proceeding Ultrasonic Symp.*, 677–682, 1988.
- [8] R. Gr. Maev, “Scanning acoustic microscopy of polymeric and biological substances”, *Tutorial Archives of Acoustics, Poland*, 13, N 1-2, 13–43, 1988.
- [9] R. Gr. Maev, V.M. Levin, “Principles of local sound velocity and attenuation measurements using transmission acoustic microscope”, *IEEE Trans. Ultrason. Ferroelec. Freq. Contr.*, 44, N6, 1224–1231, 1997.
- [10] R. Gr. Maev, S.A. Titov, “Measurement method based on scanning Doppler continuous wave acoustic microscope”, *Topics on Nondestructive Evaluation Series*, 3, ASNT Publication, 343–350, 1998.
- [11] S. Titov and R. Maev, “V(X,T) acoustic microscopy method for leaky surface acoustic waves parameters measurements”, *Proc. IEEE Ultrason. Symp.*, 607–610, 2000.
- [12] J. Kushibiki and N. Chubachi, “Material characterization by line–focus–beam acoustic microscope”, *IEEE Trans. Sonics and Ultrasonics*, SU–32, 189–212, 1985.
- [13] A. Atalar, H. Koymen, A. Bozkurt and G. Yaralioglu, “Lens geometries for quantitative acoustic microscopy”, in book *Advances in acoustic Microscopy*, 1st, New York: Plenum Press, 117–151, 1995.
- [14] K. Liang, G. Kino and B. Khuri–Yakub, “Material characterization by the inversion of V(z)”, *IEEE Trans. Sonics and Ultrasonics*, SU–32, 213–224, 1985.
- [15] K. Kushibiki, Y. Ono, Y. Ohashi and M. Arakawa, “Development of the line–focus–beam ultrasonic material characterization system”, *IEEE Trans. Ultrason. Ferroelec. Freq. Contr.*, 49, 99–113, 2002.
- [16] K. Yamanaka, “Surface acoustic waves measurements using an impulsive converging beam”, *J. Appl. Phys.*, 54, N 8, 4323–4329, 1983.
- [17] D. Xiang, N. Hsu and G. Blessing, “The design, construction and application of a large aperture lens–less line–focus PVDF transducer”, *Ultrasonics*, 34, N 6, 641–647, 1996.
- [18] S. Titov and R. Maev, “Doppler continuous wave scanning acoustic microscope”, *Proc. of IEEE Ultrason. Symp.*, 713–718, 1997.
- [19] Y. Lee and S. Cheng, *Measuring Lamb dispersion curves of a bi-layered plate and its application on material characterization of*

- coating. IEEE Trans. Ultrason. Ferroelec. Freq. Contr., 48, 830–837, 2001.
- [20] M. Nadal, P. Lebrun and C. Gondard, “Prediction of the impulse response of materials using a SAM technique in the MHz frequency range with a lensless cylindrical–focused transducer”, Ultrasonics, 36, 505–512, 1998.
- [21] R. Vines, S. Tamura and J. Wolfe, “Surface acoustic wave focusing and induced Rayleigh waves”, Phys. Rev. Lett., 74, 2729–2732, 1995.
- [22] A. Every, A. Maznev and G. Briggs, “Surface response of a fluid loaded anisotropic solid to an impulsive point source: application to scanning acoustic microscopy”, Phys. Rev. Lett., 79, N13, 2478–2481, 1997.
- [23] M. Hauser, R. Weaver and J. Wolfe, “Internal diffraction of ultrasound in crystals: phonon focusing at long wavelengths”, Phys. Rev. Lett., 68, N 17, 2604–2607, 1992.
- [24] M. Pluta, M. Schubert, J. Jahny and W. Grill, “Angular spectrum approach for the computation of group and phase velocity surface of acoustic waves in anisotropic materials”. Ultrasonics, 38, 232–236, 2000.
- [25] D. Alleyne and P. Cawley, “A two–dimensional Fourier transform method for the measurement of propagating multimode signals”, J. Acoust. Soc Am., 89, 1159–1168, 1991.
- [26] D. Fei and D. Chimenti, “Rapid dispersion curve mapping and material property estimation in plates”, Review of Progress in QNDE, 1368 – 1375, 2000.
- [27] D. Fei and D. Chimenti, “Complex transducer point model of focused–beam property estimation in plates”, Review of Progress in QNDE, 1377 – 1384, 2001.
- [28] Titov S.A., Maev R.G. and Bogachenkov A.N. (2003) “Wide-aperture, line-focused ultrasonic material characterization system based on lateral scanning”, IEEE Trans. Ultrason. Ferroelec. Freq. Contr., 50, N5 (in press)